the plant journal

SEB Society for Experimental Biology

The Plant Journal (2017) **92,** 386–399 doi: 10.1111/tpj.13660

Alteration of cell wall xylan acetylation triggers defense responses that counterbalance the immune deficiencies of plants impaired in the β-subunit of the heterotrimeric G-protein

Viviana Escudero[1,2,†], Lucía Jordá[1,2,†], Sara Sopeña-Torres[1], Hugo Mélida[1], Eva Miedes[1,2], Antonio Muñoz-Barrios[1,2], Sanjay Swami[1,2], Danny Alexander[3], Lauren S. McKee[4], Andrea Sánchez-Vallet[1,2,‡], Vincent Bulone[4,5], Alan M. Jones[6,7] and Antonio Molina[1,2,*]

[1]*Centro de Biotecnología y Genómica de Plantas, Universidad Politécnica de Madrid (UPM) – Instituto Nacional de Investigación y Tecnología Agraria y Alimentaria (INIA), Campus de Montegancedo UPM, 28223 Pozuelo de Alarcón (Madrid), Spain,*

[2]*Departamento de Biotecnología-Biología Vegetal, Escuela Técnica Superior de Ingeniería Agronómica, Alimentaría y de Biosistemas, Universidad Politécnica de Madrid (UPM), 28040 Madrid, Spain,*

[3]*Metabolon Inc., 617 Davis Drive, Suite 400, Durham, NC 27713, USA,*

[4]*Royal Institute of Technology (KTH), School of Biotechnology, Division of Glycoscience, AlbaNova University Center, SE-106 91 Stockholm, Sweden,*

[5]*ARC Centre of Excellence in Plant Cell Walls and School of Agriculture, Food and Wine, The University of Adelaide, Waite Campus, Urrbrae, SA 5064, Australia,*

[6]*Department of Biology, University of North Carolina, Chapel Hill, NC, 27599-3280, USA, and*

[7]*Department of Pharmacology, University of North Carolina, Chapel Hill, NC, 27599-3280, USA*

Received 31 March 2017; revised 10 July 2017; accepted 2 August 2017; published online 9 August 2017.
*For correspondence (e-mail antonio.molina@upm.es).
[†]These authors contributed equally to this work.
[‡]Present address: Plant Pathology Group, Institute of Integrative Biology, ETH Zurich, Zurich, Switzerland.

SUMMARY

Arabidopsis heterotrimeric G-protein complex modulates pathogen-associated molecular pattern-triggered immunity (PTI) and disease resistance responses to different types of pathogens. It also plays a role in plant cell wall integrity as mutants impaired in the Gβ- (*agb1-2*) or Gγ-subunits have an altered wall composition compared with wild-type plants. Here we performed a mutant screen to identify suppressors of *agb1-2* (*sgb*) that restore susceptibility to pathogens to wild-type levels. Out of the four *sgb* mutants (*sgb10*–*sgb13*) identified, *sgb11* is a new mutant allele of *ESKIMO1* (*ESK1*), which encodes a plant-specific polysaccharide *O*-acetyltransferase involved in xylan acetylation. Null alleles (*sgb11*/*esk1-7*) of *ESK1* restore to wild-type levels the enhanced susceptibility of *agb1-2* to the necrotrophic fungus *Plectosphaerella cucumerina BMM* (*PcBMM*), but not to the bacterium *Pseudomonas syringae* pv. *tomato* DC3000 or to the oomycete *Hyaloperonospora arabidopsidis*. The enhanced resistance to *PcBMM* of the *agb1-2 esk1-7* double mutant was not the result of the re-activation of deficient PTI responses in *agb1-2*. Alteration of cell wall xylan acetylation caused by *ESK1* impairment was accompanied by an enhanced accumulation of abscisic acid, the constitutive expression of genes encoding antibiotic peptides and enzymes involved in the biosynthesis of tryptophan-derived metabolites, and the accumulation of disease resistance-related secondary metabolites and different osmolites. These *esk1*-mediated responses counterbalance the defective PTI and *PcBMM* susceptibility of *agb1-2* plants, and explain the enhanced drought resistance of *esk1* plants. These results suggest that a deficient PTI-mediated resistance is partially compensated by the activation of specific cell-wall-triggered immune responses.

Keywords: heterotrimeric G-protein, AGB1, *agb1-2*, plant cell wall, xylan, necrotrophic fungi, immunity, pathogen-associated molecular pattern, *Plectosphaerella cucumerina*, *Arabidopsis thaliana*.

INTRODUCTION

Heterotrimeric G-proteins couple extracellular signals to changes in intracellular responses in amoebae, fungi, yeasts, plants and animals (Temple and Jones, 2007; Urano *et al.*, 2013). In animals, the heterotrimeric G-protein complex consists of Gα-, Gβ- and Gγ-subunits that become activated upon ligand binding to membrane-bound G-protein-coupled receptors (GPCRs). GPCRs catalyze nucleotide exchange on Gα-subunits upon ligand perception (Oldham and Hamm, 2008), provoking the release of the Gβγ heterodimer from the trimer. The activated Gα and Gβγ interact with downstream effectors to transduce the signal. While metazoans often possess multiple genes encoding the G-protein subunits, the heterotrimer is less variable in plants. For example, Arabidopsis has only one canonical Gα-subunit (*GPA1*), one Gβ-subunit (*AGB1*) and three Gγ-subunits (*AGG1*, *AGG2* and *AGG3*). Arabidopsis also has three atypical extra-large G-proteins (XLG1–XLG3) that interact with Gβγ (Zhu *et al.*, 2009; Chakravorty *et al.*, 2015; Maruta *et al.*, 2015; Urano *et al.*, 2016). The Arabidopsis G-protein complex is maintained in its inactive state by the *At*RGS1 protein, whose agonist-induced endocytosis leads to sustained activation of the heterotrimer (Chen *et al.*, 2003; Urano *et al.*, 2013; Liao *et al.*, 2017).

Heterotrimeric G-proteins modulate many plant developmental processes and, as such, the loss- and gain-of-function mutations in the different G-protein subunits lead to altered stomata, shoot and root development (Urano *et al.*, 2016). For example, *agb1* plants have modified organ morphology, such as rounder leaves and shorter siliques (Ullah *et al.*, 2003; Urano *et al.*, 2015). The size reduction of some organs in *agb1* is due to altered cell proliferation processes that also explain the shortened hypocotyls and open apical hooks of etiolated *agb1-2* seedlings (Ullah *et al.*, 2001, 2003; Wang *et al.*, 2006). The heterotrimeric G-protein complex also modulates responses to external stimuli like sensitivity to D-glucose, and thus *agb1* seedlings are hypersensitive to this sugar (Ullah *et al.*, 2001). Several extragenic dominant *sgb* alleles [*s*uppressor of *G*-protein *b*eta1 (*agb1-2*); *sgb1-sgb8*] were identified that rescued the hypocotyl length and apical hook opening phenotypes of *agb1-2*: *SGB1* encodes a Golgi-localized hexose transporter that restores *agb1-2* sugar hypersensitivity (Wang *et al.*, 2006), while *SGB3* encodes an acireductone dioxygenase 1 (Friedman *et al.*, 2011).

The heterotrimeric G-protein complex is an essential component of Arabidopsis immune responses and resistance to pathogens with distinct colonization styles. Single (*agb1-2*) and double (*agg1 agg2*) mutants are highly susceptible to a wide range of pathogens. These include both necrotrophic (e.g. *Plectosphaerella cucumerina BMM*, *PcBMM*), biotrophic (e.g. *Golovinomyces cichoracearum*) and vascular (e.g. *Fusarium oxysporum*) fungi, bacteria (e.g. *Pseudomonas syringae* DC3000 or *P. aeruginosa*) and viruses (Llorente *et al.*, 2005; Trusov *et al.*, 2006; Ishikawa, 2009; Lorek *et al.*, 2013; Torres *et al.*, 2013; Cheng *et al.*, 2015; Brenya *et al.*, 2016). The heterotrimeric G-protein complex operates in the pathogen-associated molecular pattern (PAMP)-triggered immunity (PTI) pathway, downstream of the recognition of PAMPs by their counterpart pattern recognition receptors (PRRs). Several components of the G-protein complex interact with some PRRs (Aranda-Sicilia *et al.*, 2015; Tunc-Ozdemir *et al.*, 2016; Tunc-Ozdemir and Jones, 2017). In *agb1-2* and *agg1 agg2* plants treated with PAMPs, such as the bacterial flg22 and elf18, or fungal chitin, the activation of early PTI responses is reduced compared with wild-type plants. Among these PTI are the production of reactive oxygen species (ROS) by the NADPH oxidase RbohD, the phosphorylation of mitogen-activated protein kinases (e.g. MPK3, MPK6 and MPK4/11) and the expression of PTI marker genes (Liu *et al.*, 2013; Liang *et al.*, 2016). The atypical XLG2 subunit is also involved together with AGB1 and AGG1/2 in the regulation of PTI by attenuating proteasome-mediated degradation of BIK1 kinase, which phosphorylates and activates RbohD, allowing optimum immunity induction (Liang *et al.*, 2016). Moreover, activation of PTI seems to occur through the phosphorylation of the negative regulator AtRGS1 by some RLKs upon ligand recognition (Tunc-Ozdemir *et al.*, 2016).

The Arabidopsis heterotrimeric G-protein complex plays a function in the determination of plant cell wall composition (Klopffleisch *et al.*, 2011; Delgado-Cerezo *et al.*, 2012). The role of plant cell wall structure in plant immunity and disease resistance has been previously described in mutants with altered wall-associated enzymes that show modified defensive responses (Brutus *et al.*, 2010; Lionetti *et al.*, 2012; Miedes *et al.*, 2014). For example, the *irx1-6* plants, impaired in the biosynthesis of cellulose in secondary cell walls, convey enhanced resistance to *PcBMM*, *Botrytis cinerea*, *G. cichoracearum and Hyaloperonospora arabidopsidis*. *irx1-6*-mediated resistance results from the accumulation of abscissic acid (ABA) and activation of the ABA signaling pathway, and the accumulation of antimicrobial peptides [e.g. thionins and lipid transfer proteins (LTPs)] and tryptophan-derived metabolites (Chen *et al.*, 2005; Hernandez-Blanco *et al.*, 2007). The cell walls of the *PcBMM* hypersusceptible mutants, such as *agb1-2* and *agg1 agg2*, have minor alterations in their wall composition, i.e. putative modifications of xyloglucan or xylan structures compared with wild-type, but these changes significantly impact disease resistance (Sánchez-Rodríguez *et al.*, 2009; Delgado-Cerezo *et al.*, 2012).

Limited information is available about heterotrimeric G-protein complex downstream effectors and scaffold proteins regulating immune responses, with the exception of

RACK1 (Klopffleisch *et al.*, 2011; Cheng *et al.*, 2015; Urano *et al.*, 2015). To identify additional components, we sought suppressors of *agb1-2* (*sgb*) susceptibility to *PcBMM* and identified four mutants (*sgb10*–*sgb13*) that restored to wild-type resistance levels the enhanced susceptibility of *agb1-2* to this fungus. Here, we show that *sgb11* corresponds to a new mutant allele of *ESKIMO1*, which encodes a polysaccharide *O*-acetyltransferase involved in plant cell wall xylan acetylation (Urbanowicz *et al.*, 2014). Our data demonstrate that modification of the degree of xylan acetylation in plant cell walls is sufficient to trigger immune responses that overcompensate *agb1-2*-deficient PTI. These activated defensive responses are sufficient to restore the enhanced susceptibility of *agb1-2* to *PcBMM* to wild-type resistance levels.

RESULTS

sgb10–*sgb13* mutants restore to wild-type levels the hypersusceptibility of *agb1-2* to *PcBMM*

We first investigated the resistance to *PcBMM* of *sgb1*–*sgb8* gain-of-function suppressors identified in a screen to restore to wild-type the *agb1-2* hypocotyl-associated phenotypes (Wang *et al.*, 2006; Friedman *et al.*, 2011). Three-week-old wild-type and *agb1-2* plants, the *sgb agb1-2* double mutants and the *irx1-6* cell wall mutant, included as a *PcBMM* resistance control, were inoculated with fungal spores, and the progression of the infection was determined by macroscopic evaluation of disease rating (DR) at different days post-inoculation (dpi; Figure S1a). None of the *sgb agb1-2* double mutants was able to fully suppress *agb1-2* hypersusceptibility to *PcBMM*, which was macroscopically associated with a profuse necrosis of leaves and petioles that eventually led to plant decay and death (Figure S1b; Delgado-Cerezo *et al.*, 2012; Ramos *et al.*, 2013). Therefore, we concluded that the *sgb1*–*sgb8* mutations were not able to restore *agb1-2*-defective disease resistance to *PcBMM*.

These results prompted us to perform another suppressor screen of *agb1-2* to isolate mutants restoring to wild-type levels the deficient resistance to *PcBMM* of *agb1-2* plants. About 15 000 plants of an ethyl methanesulfonate-mutagenized population of *agb1-2* were inoculated with *PcBMM*, and disease progression was macroscopically evaluated at different dpi. Those plants that survived *PcBMM* infection or showed significantly reduced symptoms of necrosis compared with *agb1-2* (at 10–15 dpi) were selected as putative *sgb* mutants. Their progenies were generated and inoculated with *PcBMM* to further validate the *sgb* phenotypes, and four *sgb agb1-2* (*sgb10*–*sgb13*) double mutants were selected. Fungal biomass at 3 dpi in *sgb11/sgb13 agb1-2* was similar to that of wild-type plants (Col-0), whereas in *sgb10 agb1-2* plants it was similar to that of *irx1-6*-resistant plants (Figure 1a). Disease symptoms at 13 dpi were also reduced in the four *sgb agb1-2* mutants compared with the *agb1-2* DR values (Figure 1b). None of the selected *sgb* mutants fully restored to wild-type levels the developmental phenotypes associated with the *agb1*-2 mutation, such as leaf size and morphology and plant height and architecture (Figure 1c). Therefore, we concluded that the identified *sgb* suppressors have a direct impact on the immune responses regulated by *AGB1*, while partially interfering with the developmental processes controlled by *AGB1*.

SGB11 encodes ESKIMO1 (ESK1), a specific polysaccharide *O*-acetyltransferase of the TBL protein family involved in xylan acetylation

To determine the genetic interaction between *sgb11* and *agb1-2*, we obtained the *sgb11* single mutant by crossing *sgb11 agb1-2* with Col-0 wild-type plants, and we found that the enhanced resistance of the *sgb11* mutant was linked to its characteristic developmental phenotype: dwarf and greener plants with reduced height and branching (Figure 1c). To map this recessive mutation, *sgb11* plants were crossed with La-0 plants to generate a segregating F2 population. Fine mapping located the *SGB11* gene to a region of 200 kb on chromosome 3 between the genetic markers *AthCDC2BG* (76.14 cM) and *nga707* (78.25 cM; Figure 2a; Table S2). Full genome sequencing of *sgb11* was performed, and a G to A mutation transition was found in the coding sequence of the *ESKIMO1* (*ESK1*; A*t3g55990*) gene. This mutation resulted in a premature stop codon (W262U) and a truncated protein of 261 amino acids, which lacks the DUF231 (domain of unknown function 231; Figure 2b). This domain is present in the 46 members of a large protein family called TRICHOME BIREFRINGENCE LIKE (TBL) to which ESK1 belongs (Bischoff *et al.*, 2010; Figure S2; Table S4). *ESK1* encodes a plant-specific polysaccharide *O*-acetyltransferase that is involved in xylan acetylation (Urbanowicz *et al.*, 2014), and has also been described as a key negative regulator of freezing, salt tolerance and water economy (Xin *et al.*, 2007; Bouchabke-Coussa *et al.*, 2008), as *ESK* mutant alleles (*esk1-1* to *esk1-6*) show enhanced tolerance to these abiotic stresses. The TBL family includes proteins like TBL26 that show a glucose-induced expression dependent on AGB1 (Grigston *et al.*, 2008), and a significant number of genes differentially regulated upon pathogen infection (Figure S2).

To confirm that *sgb11* is a novel *ESK1* allele, we crossed *sgb11* with the *esk1-5* allele (SALK_089531; Bouchabke-Coussa *et al.*, 2008), and found that all the F1 and F2 plants were phenotypically identical to the parental ones and show a characteristic dwarf phenotype with greener leaves (Figure 2b and c). In addition, F1 plants (*esk1-5*$^{+/-}$ *sgb11*$^{-/+}$) and the *esk1-5* mutant allele exhibited a lower *PcBMM* biomass determined by quantitative polymerase chain reaction (qPCR) than the wild-type plants (Figure 2d).

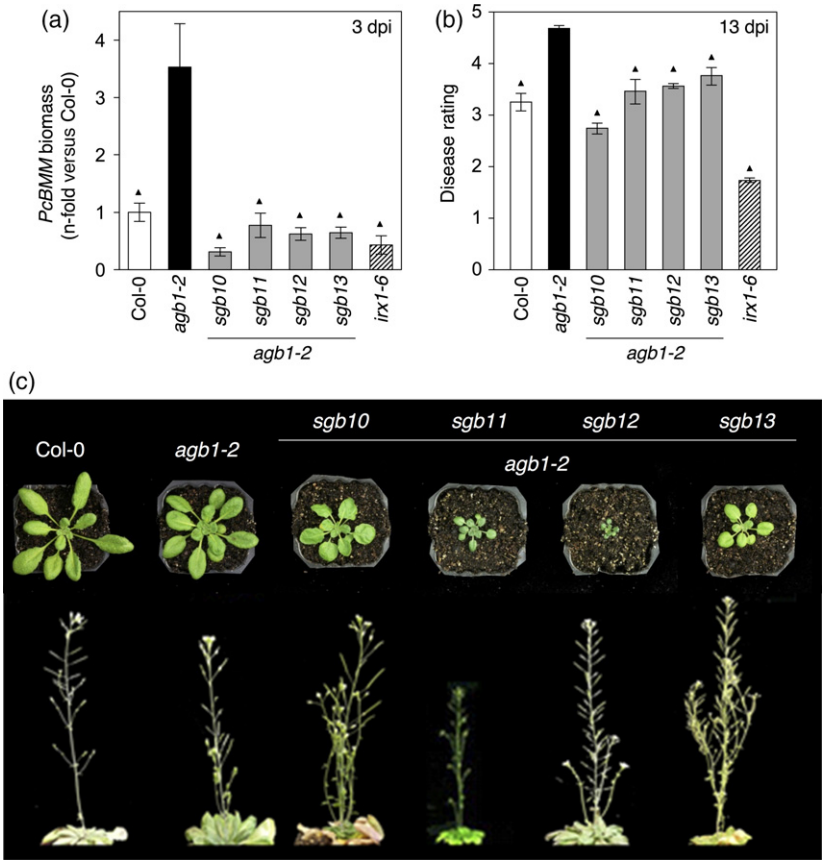

Figure 1. Identification of *sgb* mutants.
(a) Relative quantification of *PcBMM* biomass at 3 days post-inoculation (dpi). Values are normalized to Arabidopsis *UBC21* and represented as the average (± SE, $n = 2$) of the *n*-fold increase compared with Col-0 values. Values are averaged from three independent experiments.
(b) Disease rating (DR; average ± SE, $n = 10$) at 13 dpi. DR varies from 0 (non-infected plants) to 5 (dead plants; for details, see Experimental Procedures). Triangles indicate significant differences compared with *agb1-2* values (Student's *t*-test analysis, $P < 0.05$).
(c) Rosette of 4-week-old plants and 6-week-old plants architecture.

These results confirmed the genetic nature of the *sgb11* mutation that we accordingly renamed *esk1-7* allele (Figure 2d). The resistance to *PcBMM* of *esk1-7* single allele was similar to that of *esk1-5* and *irx1-6* plants, but significantly higher than that of *sgb11 agb1-2* double mutant (Figure 2d). *esk* alleles were described as *irregular xylem* (*irx*) mutants with alterations in the shape and structure of xylem cells of the vascular tissues (Lefebvre *et al.*, 2011), which have been also reported in *irx1-6* plants (Hernandez-Blanco *et al.*, 2007).

As shown in Figures 1c and S3, the *esk1-7* mutation did not restore *agb1-2*-associated developmental phenotypes to those observed in wild-type plants (Wang *et al.*, 2006; Friedman *et al.*, 2011; Urano *et al.*, 2016). Some of these *agb1*-associated phenotypes were even enhanced (e.g. reduced plant height and silique length) in the *esk1-7 agb1-2* plants compared with the *agb1-2* plants. By contrast, hypocotyl length and apical hook opening of dark-germinated *agb1-2* seedlings (Wang *et al.*, 2006) were partially rescued by *esk1-7* (Figure S3f and g). These data suggest that the *esk1-7* allele specifically affects disease resistance and seedling development responses, but it does not have any impact on other developmental phenotypes modulated by AGB1.

esk1-7/sgb11 mutation does not complement the hypersusceptibility of *agb1-2* to *P. syringae* and *H. arabidopsidis*

The *agb1-2* plants display increased susceptibility to the bacterium *P. syringae* pv. *tomato* DC3000 (*Pto*; Liu *et al.*, 2013; Torres *et al.*, 2013). We determined whether the *esk1-7* mutation restored the defense response of *agb1-2* to *Pto* by spray-inoculating Col-0, *agb1-2*, *agb1-2 esk1-7* and *esk1-7* plants with this bacterium. The *fls2* mutant, impaired in FLS2 PRR required for flg22 PAMP perception and bacterial resistance (Zipfel *et al.*, 2004), and the *cpr5* plants displaying constitutive activation of the salicylic acid (SA) pathway (Bowling *et al.*, 1997) were included as susceptible and resistance controls, respectively. As shown in Figure 3a, *Pto* growth in *esk1-7 agb1-2* was similar (at 2 dpi) or enhanced (at 4 dpi) in comparison to that determined in *agb1-2*. Bacterial growth in the *esk1-7* single mutant was significantly lower than that in *agb1-2* and *esk1-7 agb1-2*, and quite similar to that determined in Col-0 wild-type plants, which supported lower bacterial growth than *agb1-2* plants (Figure 3a), as previously described (Liu *et al.*, 2013; Torres *et al.*, 2013). These data indicate that impairment of *ESK1* is not sufficient to compensate *agb1-2* hypersusceptibility to *Pto*.

Figure 2. Map-based cloning of *SGB11* gene.
(a) Fine mapping of *sgb11* mutation on chromosome 3, between the indicated markers into artificial chromosome F27K19. The number of genetic recombinants is indicated in red.
(b) Gene model of *ESKIMO1* locus (At3g55990), showing the N-terminal and DUF231 domains, and *esk1* alleles.
(c) Morphological phenotypes of wild-type plants, *sgb11*, *esk1-5* and the hemicygote *esk1-5*$^{+/-}$ *sgb11*$^{-/+}$.
(d) Quantification of fungal *PcBMM* biomass at 5 days post-inoculation (dpi). *PcBMM.* biomass was determined by quantitative polymerase chain reaction (qPCR) quantification of *Pc β-tubulin* and Arabidopsis *UBC21* gene expression. Values are given as the average of the *n*-fold compared with wild-type plants. *irx1-6* was included as resistant control. Black triangles and asterisks indicate significant differences compared with *agb1-2* and Col-0, respectively (Student's *t*-test analysis, $P < 0.05$). This experiment has been performed three times with similar results.

Next, we tested whether resistance to the biotrophic oomycete *H. arabidopsidis* (Noco2 isolate) could be altered in the *esk1-7* mutant. Twelve-day-old seedlings from Col-0, *agb1-2*, *agb1-2 esk1-7* and *esk1-7* genotypes were inoculated, and disease was estimated at 7 dpi by determining conidiospore production per mg fresh weight (FW). In these analyses were included *NahG* transgenic plants, which do not accumulate SA and are hypersusceptible to this oomycete, and L*er* plants that harbor a resistance gene

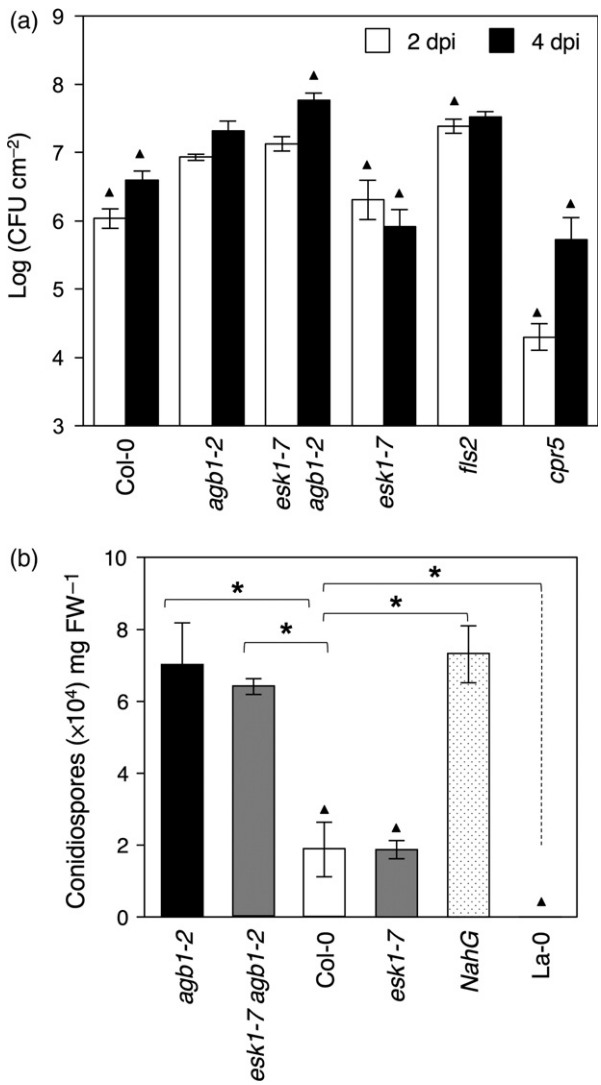

Figure 3. Resistance of *esk1-7* plants to *Pseudomonas syringae* and *Hyaloperonospora arabidopsidis*.
(a) Quantification of bacterial growth at 2 and 4 days post-inoculation (dpi). Values represent the mean (± SE) of three independent experiments. Two-tailed Student's *t*-tests for pairwise comparisons of infected plants with *agb1-2* plants (▲ $P < 0.05$) were conducted.
(b) Conidiospores of *H. arabidopsidis* (Noco2) per mg of leaf fresh weight (FW) at 7 dpi. Black triangles and asterisk indicate genotypes with significant differences in their level of resistance compared with *agb1-2* and Col-0 plants, respectively (Student's *t*-test analysis, $P < 0.05$). These experiments have been performed three times with similar results.

(*RPP5*) that confers resistance to the isolate tested (Delaney *et al.*, 1994; Parker *et al.*, 1997). *agb1-2* plants were highly susceptible to the oomycete, as evidenced by a higher conidiospores/mg FW value for *agb1-2* plants than for wild-type plants (Figure 3b). The *esk1-7* mutation did not suppress *agb1-2*-enhanced susceptibility to this pathogen, and *esk1-7* resistance was comparable to that of Col-0 plants (Figure 3b). These data indicate that *esk1-7* disease resistance to *H. arabidopsidis* was not altered.

The *esk1-7* mutation does not fully restore to wild-type levels the defective PTI responses of *agb1-2* plants

Because the heterotrimeric G-protein is a key PTI component (Liu *et al.*, 2013; Cheng *et al.*, 2015; Liang *et al.*, 2016; Tunc-Ozdemir *et al.*, 2016), we studied the activation of early immune defense responses in *esk1-7* plants upon treatment with the bacterial PAMP flg22 or a spore extract of *PcBMM* that contained a mixture of PAMPs (Jordá *et al.*, 2016). The ROS production in *agb1-2* plants treated with flg22 or *PcBMM* extract was impaired, and it was almost similar to that of the *fls2* and *cerk1* mutants, which lacks the FLS2 and CERK1 PRRs required for the recognition of flg22 and fungal chitin PAMPs, respectively, and which did not produce any ROS (Figures 4a and S4a). Notably, this defective ROS production of *agb1-2* plants was not restored to wild-type levels in *agb1-2 esk1-7* plants. In addition, ROS production in the *esk1-7* single mutant and in the *irx1-6* control plants was reduced compared with that in wild-type plants (Figures 4a and S4a).

We next investigated the phosphorylation of MPK3/MPK6/MPK4/MPK11 in plants treated with flg22 or *PcBMM* extract, and found that the defective phosphorylation of MPKs in *agb1-2* was partially restored to wild-type levels in the *agb1-2 esk1-7* plants, whereas the phosphorylation of MAPKs in *esk1-7*, *irx1-6* and wild-type plants was almost identical and contrasted with the null phosphorylation observed in *fls2* and *cerk1* mutants (Figures 4b and S4b). The defective upregulation of PTI marker genes (e.g. *CYP81F2* and *WRKY33*) in the *agb1-2* mutant upon flg22 or *PcBMM* extract treatment, as determined by reverse transcriptase (RT)-qPCR, was not fully restored to wild-type levels in the *agb1-2 esk1-7* plants (Figures 4c and S4c). In the *esk1-7* plants treated with *PcBMM* spore extract and in the *irx1-6* flg22-treated plants, induction of *WRKY33* and *CYP81F2* were slightly enhanced compared with wild-type plants, whereas induction of these genes was impaired in the control *fls2* mutant and in *cerk1* plants, with the exception of *WRKY33* expression (Figures 4c and S4c). Together, these data indicate that the defective PTI responses of *agb1-2* plants were not fully restored to wild-type levels by the *esk1-7* mutation, with the exception of MPKs phosphorylation. These data strongly support the hypothesis that *esk1-7*-mediated resistance is not associated with an enhanced upregulation of PTI.

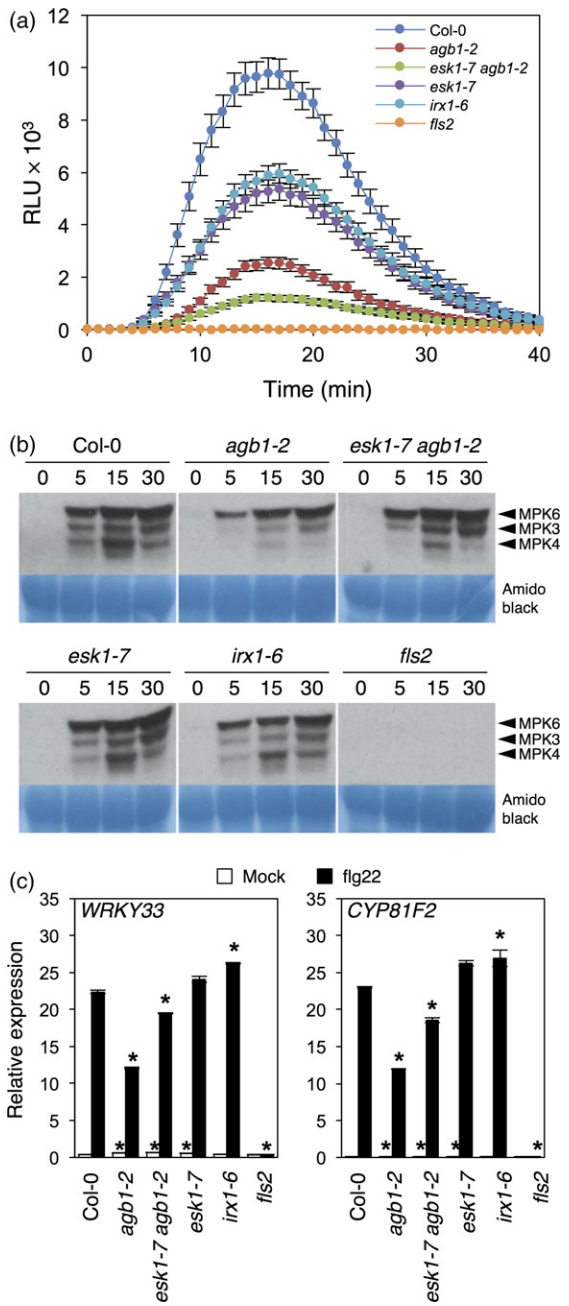

Figure 4. *esk1-7* cannot restore *agb1-2*-defective pattern-triggered immunity (PTI) response upon flg22 treatment.

(a) Reactive oxygen species (ROS) production, represented as relative luminescence units (RLU × 10^3), after flg22 (100 nM) treatment. Values are means (± SE, $n = 14$).

(b) Mitogen-activated protein kinase (MAPK) activation upon application of flg22. The phosphorylation of MPKs was determined at the indicated time points by Western blot using the Phospho-p44/42 MAPK (Erk1/2) (Thr202/Tyr204) antibody. Amido black-stained membranes are shown to assess equal loading.

(c) Quantitative reverse transcriptase-polymerase chain reaction (qRT-PCR) analyses of PTI-induced genes in mock or flg22-treated seedling (60 min). Relative expression levels to the *UBC21* gene are shown. Values are means (± SE, $n = 2$). Asterisks indicate significant differences compared with Col-0 plants (Student's *t*-test, $P < 0.05$). These experiments have been performed three times with similar results.

Because *esk1-7* and *irx1-6* plants have a reduced production of ROS upon PAMP treatment, and ROS regulates cell death formation (Torres, 2010), we determined the induction of cell death and ROS production by trypan blue and 3,3′-diaminobenzidine staining, respectively, in *PcBMM*-inoculated leaves from 3-week-old plants. As shown in Figure S5, cell death and, to a lesser extent, ROS production were reduced in the *esk1-7* plants compared with wild-type plants. Moreover, cell death produced by *PcBMM* infection was significantly reduced in the *agb1-2 esk1-7* compared with *agb1-2* plants (Figure S5a and b), further supporting the enhanced resistance of *agb1-2 esk1-7* plants to the fungus.

esk1-7 plants show a constitutive accumulation of ABA and upregulation of defense-associated genes

ESK1 mutant alleles have been described to exhibit altered levels of ABA and constitutive expression of ABA-regulated genes, including some modulating plant responses to abiotic stresses (Xin *et al.*, 2007; Lefebvre *et al.*, 2011). Because the ABA-signaling pathway is critical for proper defense responses against *PcBMM* (Chen *et al.*, 2005; Hernandez-Blanco *et al.*, 2007; Sánchez-Vallet *et al.*, 2012) and is constitutively activated in the *PcBMM*-resistant *irx1-6* plants, we analyzed the expression of some ABA-mediated defense-associated genes in *agb1-2 esk1-7* and *esk1-7* plants. ABA-regulated genes, such as *RD22* and *NCED3*, or defense-related genes, like *LTP3* or *CYP79B3*, were constitutively upregulated in *agb1-2 esk1-7* and *esk1-7* plants, and their levels of expression were similar to that of *irx1-6* plants (Figure 5a; Hernandez-Blanco *et al.*, 2007). Moreover, the constitutive overexpression of ABA-regulated genes is in line with the increased levels of abscisate found in the *esk1-7* and *irx1-6* mutants in comparison to that determined in Col-0 plants (Figure S6; Chen *et al.*, 2005; Lefebvre *et al.*, 2011). Together, these data suggest that the enhanced resistance to *PcBMM* of *esk1-7* plants is due to the activation of the ABA pathway and the expression of genes encoding antimicrobial peptides (e.g. LTP3) and enzymes involved in the synthesis of tryptophan-derived metabolites (e.g. CYP79B3). These peptides and metabolites have antibiotic activity against *PcBMM* (Hernandez-Blanco *et al.*, 2007; Sanchez-Vallet *et al.*, 2010). By contrast, in uninfected *esk1-7* and *esk1-7 agb1-2* plants we did not detect constitutive expression of genes regulated by defense hormones like SA, ethylene, jasmonic acid or ethylene + jasmonic acid (*PR1*, *PR4*, *LOX2* and *PDF1.2*, respectively; Figure S7).

Constitutive activation of ABA signaling results in an enhanced tolerance to drought (Chen *et al.*, 2005; Bouchabke-Coussa *et al.*, 2008) and, accordingly, *irx1-6* plants show enhanced recovery from water deprivation followed by re-watering (Hernandez-Blanco *et al.*, 2007). We tested whether *esk1-7* might have a similar phenotype to that of *irx1-6*. Three-week-old soil-grown Col-0, *esk1-7*, *irx1-6*, *agb1-2* and *agb1-2 esk1-7* plants and the control *aba1-6* mutant were restricted completely from water for 21 days, then the wilted plants were re-watered for 7 days and the number of surviving plants was scored. As shown in Figure S8, *esk1-7*, *agb1-2 esk1-7* and *irx1-6* showed an enhanced resistance to water deprivation with a survival rate over 80%.

esk1-7 and *irx1-6* show overlapping metabolomic profiles

Because the *esk1-7* and *irx1*-6 mutants are impaired in cell wall xylan and cellulose composition, respectively, and have similar developmental phenotypes, immune responses and resistance to biotic and abiotic stresses (Hernandez-Blanco *et al.*, 2007; Xin *et al.*, 2007; Lefebvre *et al.*, 2011), we investigated whether the *irx1-6* allele complemented *agb1-2*-enhanced susceptibility to *PcBMM*. We generated *agb1-2 irx1-6* plants that were inoculated with *PcBMM*, and we found that the *irx1-6* allele, similar to the *esk1-7* allele, restored to wild-type levels the enhanced susceptibility of *agb1-2* plants to the fungus (Figure S9).

Independent transcriptomic analyses of *esk1-7* and *irx1*-6 were performed previously under different growth conditions, and some constitutively upregulated genes were found to be common to both mutants (Figure 6a; Hernandez-Blanco *et al.*, 2007; Xin *et al.*, 2007). To further characterize specific or common defensive responses in *esk1-7* and *irx1-6* plants, we performed a global comparative metabolomic analysis on 4-week-old, non-inoculated *esk1-7*, *irx1-6* and wild-type plants. Among the 320 metabolites tested, we found significant alterations in the content of 93 and 78 metabolites in *irx1-6* and *esk1-7*, respectively (Figure 5b; Table S1). Interestingly, a high degree of concordance was observed between *esk1-7/irx1-6* profiles with 55 metabolites showing similar patterns (enhanced accumulation or reduction) compared with wild-type plants (Figure 5b; Table S1). Despite these overlapping profiles, some compounds showed specific patterns (23 in *esk1-7*, and 38 in *irx1-6*; Figure 5c; Table S1), indicating that the defense responses and metabolism reprogramming were not identical in both mutants. For example, in *irx1-6*, we found an enrichment of metabolites of the tricarboxylic acid and the serine and ascorbate metabolic pathways, whereas in *esk1-7* the riboflavin/FAD, phospholipid and α-ketoglutarate-related pathways were enriched (Figure 5c; Table S1). Remarkably, some groups of metabolites associated with plant defensive responses, such as glucosinolates, benzenoides, polyamines and phenylpropanoids, were overrepresented in both mutants in comparison to wild-type plants (Figure 5c). Among these metabolites, there were several aliphatic-glucosinolates (e.g. glucoraphanin, sulforaphan and sulforphan-*N*-acetyl-cysteine) and indole-glucosinolate (e.g. indole-3-carboxylic acid), which are required for pathogen resistance (Sanchez-Vallet *et al.*,

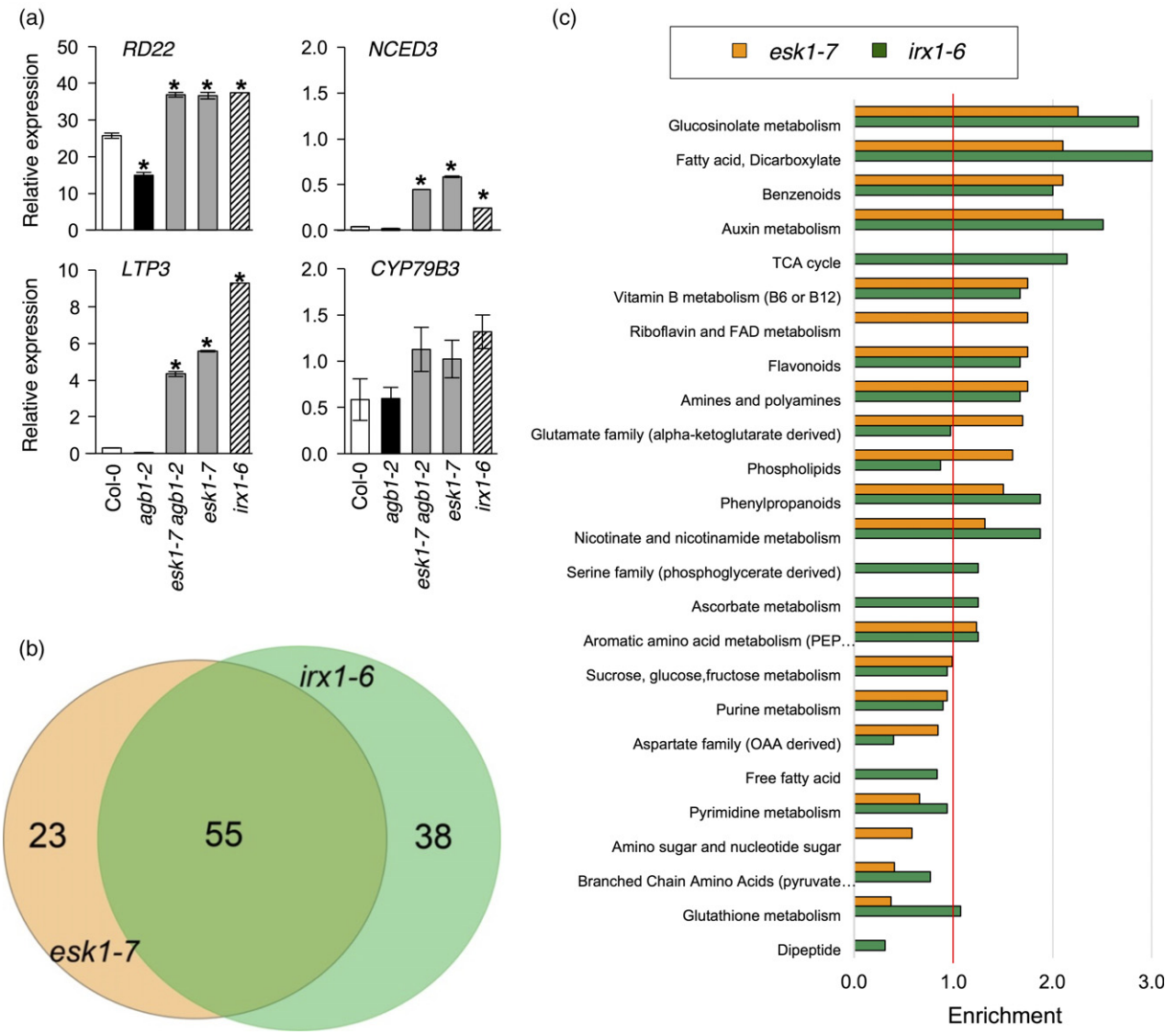

Figure 5. Defensive responses are constitutively upregulated in *esk1-7* and *irx1-6* plants.
(a) Gene expression was determined by quantitative reverse transcriptase-polymerase chain reaction (qRT-PCR) in tissues from 21-day-old untreated plants, and are represented as the average ($n = 3 \pm$ SE). Transcript levels of analyzed genes were normalized to the Arabidopsis *UBC21* gene. Asterisks indicate significant differences compared with Col-0 plants (Student's *t*-test, $P < 0.05$). These experiments have been performed three times with similar results.
(b) Comparative metabolite enrichment of *esk1-7* and *irx1-6* plants. The Venn diagram shows the number of miss-regulated metabolites identified in *esk1-7* and *irx1-6* in comparison to wild-type plants ($P < 0.1$).
(c) Metabolic pathway enrichment in *esk1-7* and *irx1-6*. Values were calculated as the number of experimentally regulated compounds ($P < 0.05$) relative to all detected compounds in a pathway, compared with the total number of experimentally regulated compounds relative to all detected compounds in the study (321). Pathways with less than three metabolites were not included in the analysis.

2010; Schlaeppi and Mauch, 2010; Fan *et al.*, 2011). The increased levels of these defensive metabolites in *esk1-7* and *irx1-6* may contribute to the generation of a hostile environment for the pathogens inhibiting their growth.

Similarly, several abiotic stress-associated metabolites, in addition to the previously described proline (Xin and Browse, 1998), accumulated in the *esk1-7* and *irx1-6* mutants compared with wild-type plants. Among them were several compounds of proline metabolism (trans-4-hydroxyproline, *N*-acetyl-proline, myo-inositol) and carbohydrates, like sucrose and galactinol, contributing to plant osmoprotection (Figure 5c; Table S1; Taji *et al.*, 2002; Szabados and Savouré, 2010). The accumulation of these metabolites would explain the enhanced resistance of these plants to dehydration (Figure S8).

esk1-7 and *agb1-2* plants show alterations in the degree of cell wall xylan acetylation

ESK1 is a polysaccharide *O*-acetyltransferase involved in xylan acetylation (Urbanowicz *et al.*, 2014), and changes in

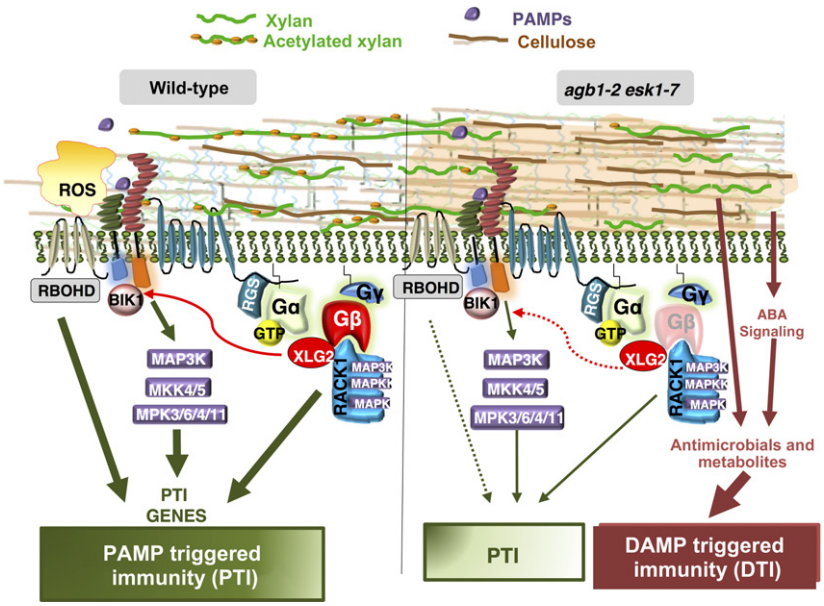

Figure 6. Cell-wall-based immunity mediated by ESK1 impairment.
In wild-type plants (left panel), pathogen-associated molecular patterns (PAMPs) perception by pattern recognition receptors (PRR) and co-receptors leads to the activation of heterotrimeric G-protein complex, which in turns modulate reactive oxygen species (ROS) production, mitogen-activated protein kinase (MAPK) phosphorylation and gene expression to positively activate pattern-triggered immunity (PTI). In *agb1-2* mutants (right panel), these responses are defective, but alterations in plant cell wall xylan acetylation caused by *esk1* mutation lead to the activation of cell wall-mediated DAMP triggered immunity (DTI) responses, which overcompensate *agb1-2*-defective PTI responses.

Arabidopsis cell wall composition have been described in the *esk1* mutant alleles (Xiong *et al.*, 2013; Yuan *et al.*, 2013). In order to determine if similar minor types of wall modifications occurred in *esk1*, rather than major wall remodeling, we monitored some cell wall carbohydrate components (cellulose, neutral sugars and uronic acids) in the rosette of 3-week-old plants, and we found no major differences between the *esk*1-7, *esk1-7 agb1-2*, *agb1-2* and wild-type plants (Figure S10). To determine the degree of xylan acetylation in the set of genotypes, methods for hemicellulose extraction and purification were used that did not involve the typical alkali treatments, which give high yield extraction but lead to extensive deacetylation of hemicelluloses. Instead, xylans were extracted using dimethylsulfoxide, as described in Hägglund *et al.* (1956). We confirmed a decreased acetic acid:xylose ratio in the *esk1-7* mutants, as reported previously (Xiong *et al.*, 2013; Yuan *et al.*, 2013), and also in the *irx1-6* cell wall mutant (Figure S11). Notably, *agb1-2* cell walls also showed a slight reduction in acetic acid:xylose ratio compared with wild-type plants, which was not restored to wild-type levels in the *esk1-7 agb1-2* plants. However, modifications in the degree of acetylation of xylan were minor, although significant, and the genotypes showed no real variability in the profile of decorated oligosaccharides produced by the xylanase enzyme, as inferred from MALDI-TOF-MS analysis (Figure S11a). These data suggest that different mutations impairing genes required for secondary cell wall formation cause subtle alterations in polysaccharide decoration that result in relevant changes in cell wall integrity.

DISCUSSION

The Arabidopsis heterotrimeric G-protein complex is a key component of PTI and broad-spectrum disease resistance responses (Llorente *et al.*, 2005; Trusov *et al.*, 2006; Ishikawa, 2009; Lorek *et al.*, 2013; Torres *et al.*, 2013; Cheng *et al.*, 2015; Brenya *et al.*, 2016). AGB1 and AGG1 + AGG2 subunits are essential for the activation of PTI, and activation of heterotrimeric G function in immunity depends on the phosphorylation of the AtRGS1 negative regulator by some PRRs upon ligand recognition (Liu *et al.*, 2013; Aranda-Sicilia *et al.*, 2015; Liang *et al.*, 2016; Tunc-Ozdemir *et al.*, 2016). Therefore, it was surprising to find here that the restoration of the wild-type *PcBMM* resistance levels in *agb1-2* plants by *esk1* mutation was not the result of an effective re-activation of PTI in *agb1-2* plants, with the exception of MAPKs phosphorylation (Figures 1 and 3). Our data demonstrate that the *agb1-2* defective PTI was counterbalanced by alteration of *agb1-2* wall xylan-decoration through inactivation of the xylan-specific *O*-acetyltransferase ESK1/TBL29 (Urbanowicz *et al.*, 2014). Impairment of the *ESK1/TBL29* gene results in a slight reduction of xylan acetylation in cell walls from leaves of 3-week old *esk1-7* plants (Figure S11), that is in line with the previously described reduced xylan acetylation of the secondary cell wall of inflorescence stems from mature plants of other *esk1* alleles (Xiong *et al.*, 2013; Yuan *et al.*, 2013). These results suggest that strategies of defense to pathogens are multi-layered and, in some ways, are pathogen specific, and that only by impairing some canonical layers of defense (e.g. heterotrimeric G-protein) the relevance of additional immune responses (i.e. cell wall-mediated defense) and their role in specific-resistance responses can be determined (Figure 6; Lipka *et al.*, 2005).

Notably, in the *agb1-2 esk1-7* double mutant we found PTI-independent defensive responses that were constitutively activated, including ABA-enhanced accumulation and expression of ABA-regulated genes, the expression of

genes encoding antimicrobial peptides and enzymes required for the synthesis of tryptophan-derived metabolites, and the accumulation of defensive-associated secondary metabolites (Figure 5). The majority of the *esk1-7* constitutively activated immune responses are also upregulated in the *irx1-6* plants, and both mutants show a significant overlap in their metabolomic profiles. The *esk1-7* plants show a reduction in PAMP-triggered ROS production and in cell death upon fungal infection (Figures 4, S4 and S5), which might also contribute to slow-down *PcBMM* growth. In line with these data, impairment of the *IRX1* gene in *agb1-2 irx1-6* double mutant also resulted in a restoration of *PcBMM* resistance to wild-type levels (Figure S9). Despite the similarities between the *esk1-7* and *irx1-6* defensive responses, the *irx1-6* mutant shows enhanced resistance to several pathogens, including *H. arabidopsis* (Hernandez-Blanco *et al.*, 2007), whereas *esk1-7* resistance to this oomycete does not differ from that of wild-type plants (Figure 3b). Altogether, these results suggest that modifications in cell walls provide specificity in pathogen defense, as reported previously (Miedes *et al.*, 2014).

Effective defense against pathogens might result from alterations of the biochemical or structural properties of the cell wall in the mutants or transgenic plants, which are expected to lead to either stronger or weaker walls (Lionetti *et al.*, 2012; Miedes *et al.*, 2014). This would result in walls being generally more recalcitrant or more susceptible to degradation by cell wall-degrading enzymes secreted by fungal pathogens. For example, the deacetylation of wall polysaccharides (e.g. xylan, mannan and rhamnogalacturonan I) is a prerequisite for the enzymatic degradation of walls by most if not all microbial pathogens and saprophytes. Some specific microorganisms secrete acetyl xylan esterases (AXEs) that deacetylate polymeric xylan and xylo-oligosaccharides, as well as enzymes that deacetylate other wall components (Biely, 2012; Pawar *et al.*, 2013). Subtle cell wall modifications, such as the degree of acetylation, are therefore expected to thwart ingress of certain pathogens. Another possible explanation for the basis of pathogen specificity in plant defense mediated by cell wall integrity is the release of plant cell wall-derived signals as a product of cell wall degradation by pathogen-secreted enzymes. Among these wall-released signals are pectin-derived oligogalacturonides, which are damage-associated molecular patterns (DAMPs) that can trigger immunity (DTI responses; Ferrari *et al.*, 2013). Subtle alterations in the cell wall structure may lead to the production of different types of wall DAMPs that might activate specific wall-mediated DTI responses. In *agb1-2 esk1-7* plants, DTI could overcompensate the deficient PTI responses (Figure 6).

The relationship between cell wall acetylation and biotic/abiotic resistance is complex. Acetylation of xylans and other wall polysaccharides is essential for plant growth and plant adaptation to environmental changes (Pawar *et al.*, 2013; Busse-Wicher *et al.*, 2014; Yuan *et al.*, 2016). Three groups of plant proteins are involved in polymer *O*-acetylation: TBLs, RWAs (reduced wall acetylation) and AXY9 (altered xyloglucan 9; Gille and Pauly, 2012; Schultink *et al.*, 2015). In addition to *esk1/tbl29*, that shows enhanced disease resistance to *PcBMM* and *P. syringae* (Figures 1 and 3), other *tbl* mutants have altered immune responses. For example, *pmr5* (*tbl44*) exhibits tolerance to powdery mildew (Vogel *et al.*, 2004), and rice *tbl1 tbl2* double mutant displays enhanced susceptibility to rice blight disease (Gao *et al.*, 2017). Mutation of RWA2 results in an overall reduction of acetylation on several polymers and enhanced resistance to some pathogens, like *H. arabidopsidis* and the necrotrophic fungus *B. cinerea*, but not to *PcBMM* and the bacterium *P. syringae* (Manabe *et al.*, 2011; Pawar *et al.*, 2016). Moreover, transgenic plants overexpressing AXE enzymes form *Aspergillus niger* or *Aspergillus nidulans* have reduced xylan acetylation and increased resistance to *H. arabidopsidis* and *B. cinerea*, but not to *PcBMM* and *P. syringae* (Pogorelko *et al.*, 2013; Pawar *et al.*, 2016). Moreover, the *esk1* (*tbl29*) mutant displays freezing tolerance in the absence of cold acclimation and enhanced resistance to long periods of dehydration (Xin and Browse, 1998; Xin *et al.*, 2007; Bouchabke-Coussa *et al.*, 2008; Figure S8). Metabolic profiling confirmed that *esk1-7* accumulates high levels of stress-associated metabolites (Table S3; Xin and Browse, 1998; Lugan *et al.*, 2009). Altogether, these observations reveal the complex and diverse type of impacts that modifications of cell wall acetylation have in plant response to environmental stresses.

The G-protein pathway defines a central signaling node for cellular behaviors (Urano *et al.*, 2016). The *esk1-7* mutation does not restore defective developmental phenotypes of *agb1-2* plants like their rounder leaves and short siliques (Ullah *et al.*, 2001, 2003), whereas the defective hypocotyl length and hooks curvature of dark-grown *agb1-2* seedlings (Wang *et al.*, 2006; Friedman *et al.*, 2011) were only partially restored in *esk1-7 agb1-2* plants. This contrasted with the restoration of these phenotypes in *agb1-2* plants with extragenic gain of function suppressors (e.g. *sgb1* and *sgb3*; Wang *et al.*, 2006; Friedman *et al.*, 2011). We hypothesize that *esk1-7* is able to rescue hypocotyl length in the *agb1-2* mutant by allowing cell wall expansion, because many components such as pectins and xyloglucans are assembled in the Golgi apparatus where ESK1 is also located (Baydoun *et al.*, 1991; Yuan *et al.*, 2013). Notably, the extragenic gains of function suppressors (*sgb1–sgb8*) were not able to restore to wild-type levels *agb1-2* susceptibility to *PcBMM*, indicating that there is some degree of specificity in the signaling pathways regulated by the G-protein complex. Our data suggest that the heterotrimeric G-protein complex could have a role as a cell wall integrity regulator, mediating responses to biotic or

abiotic stresses that impact on the cell wall composition and structure. For that function, we hypothesize that the G-protein would interact with downstream effectors (e.g. PRRs) acting as cell wall integrity sensors, in a similar way as has been described for immunity (Figure 6; Aranda-Sicilia *et al.*, 2015; Liang *et al.*, 2016). The identification of these downstream effectors and wall DAMPs regulating these immune responses will contribute to better understanding of the key roles of heterotrimeric G-protein complex in plant immunity.

EXPERIMENTAL PROCEDURES

Biological materials and growth conditions

Arabidopsis plants were grown in sterilized soil, as described previously (Llorente *et al.*, 2005), or *in vitro* [Murashige and Skoog (MS) medium, as reported (Jordá *et al.*, 2016)]. The following lines (Col-0 background) were used: *agb1-2* (Ullah *et al.*, 2003); *cpr5* (Bowling *et al.*, 1997); *NahG* (Delaney *et al.*, 1994); *irx1-6* (Hernandez-Blanco *et al.*, 2007); *fls2* (Zipfel *et al.*, 2004); *cerk1-2* (Miya *et al.*, 2007); *aba1-6* (Niyogi *et al.*, 1998); and *esk1-5* (Bouchabke-Coussa *et al.*, 2008).

Pathogenicity assays

Plectosphaerella cucumerina BMM inoculation and determination of disease symptoms were performed as described (Jordá *et al.*, 2016). Briefly, a suspension of 4×10^6 spores/ml of *PcBMM* was sprayed onto 17-day-old Arabidopsis. The DR scale was as follows (Jordá *et al.*, 2016): (0) no symptoms; (1) leaves with chlorosis; (2) one-two necrotic leaves; (3) three or more leaves with necrosis; (4) most of the leaves with profuse necrosis; (5) dead plant. Oligonucleotides used for *PcBMM* biomass quantification are depicted in Table S3. Inoculation of plants with *H. arabidopsidis* and determination of level of infection were performed as reported, using a conidiospore suspension of 4×10^4 spores/ml of the Noco2 isolate (Llorente *et al.*, 2005). *Pseudomonas syringae* pv *tomato* was spray inoculated onto plants following described methods (Torres *et al.*, 2013). All pathogens resistance assays were performed with at least 10 plants and repeated three times.

Trypan blue and diaminobenzidine (DAB) stainings

Arabidopsis plants were spray inoculated with a *PcBMM* suspension of 4×10^6 spores/ml or water (mock), and 48 h post-inoculation (hpi) leaves were collected for trypan blue or DAB staining following procedures described in Morales *et al.* (2016). Quantification of stained areas was performed using Fiji software (Schindelin *et al.*, 2012). To quantify the stained pixel, leaves images were adjusted using Brightness/Contrast and RGB default Threshold Color methods, and stained areas were detected within the Analyze Particles function. The total leaf area was measured with Polygon Selections and Measure function. Total stained pixels were normalized to total leaf area and represented as % of total leaf surface.

Suppressor screen of *agb1-2* mutants and genetic mapping of *SGB11*

An EMS-treated (0.3% for 16 h) *agb1*-2 population (50 000 seeds) was generated. Germination efficiency of this mutagenized EMS population was approximately 80%. For *sgb* mutant screen, about 15 000 17-day-old plants grown in soil were inoculated with 4×10^6 spores/ml of *PcBMM*, and disease progression was macroscopically evaluated at different dpi. A *sgb11* (Col-0) × La-0 F2 population of 2035 individuals was generated to map the *SGB11* gene. F2 *sgb11* plants were selected based on their characteristic *i*rregular *x*ylem-like phenotype that resembles that of *irx1* (Hernandez-Blanco *et al.*, 2007). The *sgb11/esk1* mutation was mapped to chromosome 3 between markers *Ath*CDC2BG (BAC F24B22, one recombinant) and *nga707* (BAC T20N10, four recombinants), using the primers described in Table S2. To further position the *sgb11/esk1* mutation, genomic DNA from *sgb11* plants was fully sequenced using the Illumina technology (BGI, Hong Kong), and a single nucleotide transition was found in the *ESKIMO* gene (*At3g55990*).

Morphometric analyses

Arabidopsis seeds were grown in MS medium containing 1% sucrose and 0.8% phyto agar. After a 2–4 h light pretreatment, seeds were incubated in the dark at 23°C for 60 h. Hypocotyl lengths and apical hook angles from 24 plants/genotypes were quantified using ImageJ software. Traits were statistically analyzed using the Bonferroni test (ANOVA, $P < 0.05$). Forty-four-day-old Arabidopsis plants grown in white light at 175 μmol m^{-2} sec^{-1} under short day conditions were used to perform all morphometric analyses. Measurements were performed on 10 plants, and the experiments were repeated twice following the procedures described by Shpak *et al.* (2004).

Evaluation of immune responses

Mitogen-activated protein kinase (MAPK) activation assays and gene expression analysis after treatment with either *PcBMM* spore extracts or 100 nM flg22 were carried out as described with 12-day-old Arabidopsis seedlings grown on liquid MS medium (Jordá *et al.*, 2016). Three-week-old plants were used to determine ROS production after treatment with *PcBMM* spore extracts or 100 nM flg22 using the luminol assay and a VariosKan Lux luminescence reader (Thermo). Oligonucleotides (designed with Primer Express 2.0; Applied Biosystems) used for detection of gene expression are described in Table S3.

Drought assays

Three-week-old soil-grown plants ($n = 8$) were restricted completely from water for 21 days. Wilted plants were then watered for 7 days, and the number of recovered plants was scored. The experiments were performed four times.

Metabolomic analysis

Tissues from 25-day-old Col-0, *esk1-7* and *irx1-6* plants ($n = 10$) were collected, ground in liquid nitrogen and lyophilized. Four biological replicates for each of these genotypes were further processed and analyzed by Metabolon (Research Triangle Park, North Carolina, USA) for global unbiased metabolite profiling as described (Ren *et al.*, 2012). Metabolites altered in *irx1-6* and *esk1-7* plants are shown in Table S1. Abscisate levels were measured in at least triplicates of each genotype (25 day old plants) by ultra-performance liquid chromatography (Waters ACQUITY) and a Thermo Scientific Q-Exactive high-resolution/accurate mass spectrometer interfaced with a heated electrospray ionization (HESI-II) source and Orbitrap mass analyzer operated at 35 000 mass resolution.

Phylogenetic analysis

Unrooted phylogenetic trees were generated using the Neighbor-Joining algorithm in MEGA5 (Tamura *et al.*, 2011), and inferred

using the Muscle method based on the full-length protein sequence of *Arabidopsis thaliana* ESKIMO1/TBL29 (*At3g55990*) and members of the TBL family (Table S4). Data from Arabidopsis eFP Browser were used for gene expression (Winter *et al.*, 2007).

Biochemical characterization of plant cell walls and analysis of xylan acetylation

Cell walls were prepared from 25-day-old Arabidopsis plants according to Bacete *et al.* (2017), and total monosaccharides, uronic acids and crystalline cellulose were determined as previously described (Mélida *et al.*, 2009). Fractions enriched in hemicellulose were obtained from cell wall material by extractions in dimethylsulfoxide (DMSO) at room temperature followed by dialysis (molecular weight cutoff 3500 Da; Spectra/Por; Spectrum Laboratories) of the DMSO-soluble fraction. The dialyzed samples were then lyophilized. A MALDI-ToF approach was utilized to analyze cell wall xylans (McKee *et al.*, 2016). Total acetic acid content in the 1 M NaOH extracts from total cell walls and DMSO hemicellulosic fractions were determined using the Acetyl-CoA Synthetase kit (Megazyme K-ACET). The xylose content of DMSO extracts was determined after the conversion of 2 M TriFluoroAcetic acid-hydrolyzed (121°C for 3 h) monosaccharides to alditol acetates (Mélida *et al.*, 2013).

ACKNOWLEDGEMENTS

This work was supported by the Spanish Ministry of Economy and Competitiveness (MINECO) grants BIO2015-64077-R and BIO2012-32910 to A.M.; The Australian Research Council Centre of Excellence in Plant Cell Walls and matching funding from KTH (grants to V.B) and NIGMS (R01GM065989) and NSF (MCB-1713880) to A.M.J. The Division of Chemical Sciences, Geosciences, and Biosciences, Office of Basic Energy Sciences of the US Department of Energy through the grant DE-FG02-05er15671 to A.M.J. funded technical support in this study. H.M. was supported by an IEF grant (SignWALLINg-624721) from the European Union, E.M. by a Juan de la Cierva Postdoctoral Fellow from MINECO, S.S. by the BRAVE Erasmus Mundi Program (European Union), and A.M.-B. was the recipient of a PIF fellow from Universidad Politécnica de Madrid. The authors thank the Molina laboratory members for useful discussion and comments on the manuscript.

CONFLICT OF INTEREST

All authors confirm that there are no conflicts of interest to declare.

SUPPORTING INFORMATION

Additional Supporting Information may be found in the online version of this article.

Figure S1. Susceptibility of *sgb* mutants to *PcBMM*.

Figure S2. Arabidopsis TLB members.

Figure S3. Morphometric analysis of *esk1-7* and *esk1-7agb1-2* plants.

Figure S4. Early defense responses of *esk1-7* and *esk1-7agb1-2* plants after treatment with *PcBMM* spore extracts.

Figure S5. *esk1-7* plants show reduced cell death and ROS production upon *PcBMM* infection.

Figure S6. Abscisate levels of *esk1-7* and *irx1-6* mutants compared with Col-0.

Figure S7. Expression of defense genes regulated by SA, JA and ET-mediated is not constitutively upregulated in *esk1-7* plants.

Figure S8. Response of *esk1-7* to drought stress.

Figure S9. *irx1-6* mutation can suppress *agb1-2* susceptibility to *PcBMM*.

Figure S10. Biochemical composition of cell wall from Col-0, *agb1-2*, *esk1-7agb1-2*, *esk1-7* and *irx1-6* plants.

Figure S11. Xylan acetylation analysis.

Table S1. Heat map of metabolites altered in *esk1-7* and *irx1-6* compared with wild-type plants

Table S2. Primers used for *sgb11/esk1* mapping.

Table S3. Primers used in this study.

Table S4. Arabidopsis TLB members.

REFERENCES

Aranda-Sicilia, M.N., Trusov, Y., Maruta, N., Chakravorty, D., Zhang, Y. and Botella, J.R. (2015) Heterotrimeric G proteins interact with defense-related receptor-like kinases in Arabidopsis. *J. Plant Physiol.* **188**, 44–48.

Bacete, L., Mélida, H., Pattathil, S., Hahn, M.G., Molina, A. and Miedes, E. (2017) Characterization of plant cell wall damage-associated molecular patterns regulating immune responses. *Methods Mol. Biol.* **1578**, 13–23.

Baydoun, E.A., Hobbs, M.C., Delarge, M.H., Farmer, M.J., Waldron, K.W. and Brett, C.T. (1991) Formation of glucuronoxylan linked to protein in plant Golgi and plasma membranes. *Biochem. Soc. Trans.* **19**, 250S.

Biely, P. (2012) Microbial carbohydrate esterases deacetylating plant polysaccharides. *Biotechnol. Adv.* **30**, 1575–1588.

Bischoff, V., Selbig, J. and Scheible, W.R. (2010) Involvement of TBL/DUF231 proteins into cell wall biology. *Plant Signal. Behav.* **5**, 1057–1059.

Bouchabke-Coussa, O., Quashie, M.L., Seoane-Redondo, J., *et al.* (2008) ESKIMO1 is a key gene involved in water economy as well as cold acclimation and salt tolerance. *BMC Plant Biol.* **8**, 125.

Bowling, S.A., Clarke, J.D., Liu, Y., Klessig, D.F. and Dong, X. (1997) The cpr5 mutant of Arabidopsis expresses both NPR1-dependent and NPR1-independent resistance. *Plant Cell*, **9**, 1573–1584.

Brenya, E., Trusov, Y., Dietzgen, R.G. and Botella, J.R. (2016) Heterotrimeric G-proteins facilitate resistance to plant pathogenic viruses in Arabidopsis thaliana (L.) Heynh. *Plant Signal. Behav.* **11**, e1212798.

Brutus, A., Sicilia, F., Macone, A., Cervone, F. and De Lorenzo, G. (2010) A domain swap approach reveals a role of the plant wall-associated kinase 1 (WAK1) as a receptor of oligogalacturonides. *Proc. Natl Acad. Sci. USA*, **107**, 9452–9457.

Busse-Wicher, M., Gomes, T.C., Tryfona, T., Nikolovski, N., Stott, K., Grantham, N.J., Bolam, D.N., Skaf, M.S. and Dupree, P. (2014) The pattern of xylan acetylation suggests xylan may interact with cellulose microfibrils as a twofold helical screw in the secondary plant cell wall of Arabidopsis thaliana. *Plant J.* **79**, 492–506.

Chakravorty, D., Gookin, T.E., Milner, M.J., Yu, Y. and Assmann, S.M. (2015) Extra-large G proteins expand the repertoire of subunits in Arabidopsis heterotrimeric G protein signaling. *Plant Physiol.* **169**, 512–529.

Chen, J.G., Willard, F.S., Huang, J., Liang, J., Chasse, S.A., Jones, A.M. and Siderovski, D.P. (2003) A seven-transmembrane RGS protein that modulates plant cell proliferation. *Science*, **301**, 1728–1731.

Chen, Z., Hong, X., Zhang, H., Wang, Y., Li, X., Zhu, J.K. and Gong, Z. (2005) Disruption of the cellulose synthase gene, AtCesA8/IRX1, enhances drought and osmotic stress tolerance in Arabidopsis. *Plant J.* **43**, 273–283.

Cheng, Z., Li, J.F., Niu, Y., *et al.* (2015) Pathogen-secreted proteases activate a novel plant immune pathway. *Nature*, **521**, 213–216.

Delaney, T.P., Uknes, S., Vernooij, B., *et al.* (1994) A central role of salicylic acid in plant disease resistance. *Science*, **266**, 1247–1250.

Delgado-Cerezo, M., Sanchez-Rodriguez, C., Escudero, V., *et al.* (2012) Arabidopsis heterotrimeric G-protein regulates cell wall defense and resistance to necrotrophic fungi. *Mol. Plant*, **5**, 98–114.

Fan, J., Crooks, C., Creissen, G., Hill, L., Fairhurst, S., Doerner, P. and Lamb, C. (2011) Pseudomonas sax genes overcome aliphatic isothiocyanate-mediated non-host resistance in Arabidopsis. *Science*, **331**, 1185–1188.

Ferrari, S., Savatin, D.V., Sicilia, F., Gramegna, G., Cervone, F. and Lorenzo, G.D. (2013) Oligogalacturonides: plant damage-associated molecular patterns and regulators of growth and development. *Front. Plant Sci.*, **4**, 49.

Friedman, E.J., Wang, H.X., Jiang, K., Perovic, I., Deshpande, A., Pochapsky, T.C., Temple, B.R., Hicks, S.N., Harden, T.K. and Jones, A.M. (2011) Acireductone dioxygenase 1 (ARD1) is an effector of the heterotrimeric G protein beta subunit in Arabidopsis. *J. Biol. Chem.* **286**, 30 107–30 118.

Gao, Y., He, C., Zhang, D., *et al.* (2017) Two trichome birefringence-like proteins mediate xylan acetylation, which is essential for leaf blight resistance in rice. *Plant Physiol.* **173**, 470–481.

Gille, S. and Pauly, M. (2012) O-acetylation of plant cell wall polysaccharides. *Front. Plant Sci.* **3**, 12.

Grigston, J.C., Osuna, D., Scheible, W.R., Liu, C., Stitt, M. and Jones, A.M. (2008) D-glucose sensing by a plasma membrane regulator of G signaling protein, AtRGS1. *FEBS Lett.* **582**, 3577–3584.

Hägglund, E., Lindberg, B. and McPherson, J. (1956) Dimethylsulphoxide, a solvent for hemicelluloses. *Acta. Chemica. Scandinavica.*, **10**, 1160–1164.

Hernandez-Blanco, C., Feng, D.X., Hu, J., *et al.* (2007) Impairment of cellulose synthases required for Arabidopsis secondary cell wall formation enhances disease resistance. *Plant Cell*, **19**, 890–903.

Ishikawa, A. (2009) The Arabidopsis G-protein beta-subunit is required for defense response against Agrobacterium tumefaciens. *Biosci. Biotechnol. Biochem.* **73**, 47–52.

Jordá, L., Sopeña-Torres, S., Escudero, V., Nuñez-Corcuera, B., Delgado-Cerezo, M., Torii, K.U. and Molina, A. (2016) ERECTA and BAK1 receptor like kinases interact to regulate immune responses in Arabidopsis. *Front. Plant Sci.* **7**, 897.

Klopffleisch, K., Phan, N., Augustin, K., *et al.* (2011) Arabidopsis G-protein interactome reveals connections to cell wall carbohydrates and morphogenesis. *Mol. Syst. Biol.* **7**, 532.

Lefebvre, V., Fortabat, M.N., Ducamp, A., North, H.M., Maia-Grondard, A., Trouverie, J., Boursiac, Y., Mouille, G. and Durand-Tardif, M. (2011) ESKIMO1 disruption in Arabidopsis alters vascular tissue and impairs water transport. *PLoS ONE*, **6**, e16645.

Liang, X., Ding, P. and Lian, K. *et al.* (2016) Arabidopsis heterotrimeric G proteins regulate immunity by directly coupling to the FLS2 receptor. *Elife*, **5**, e13568.

Liao, K.L., Jones, R.D., McCarter, P., Tunc-Ozdemir, M., Draper, J.A., Elston, T.C., Kramer, D. and Jones, A.M. (2017) A shadow detector for photosynthesis efficiency. *J. Theor. Biol.* **414**, 231–244.

Lionetti, V., Cervone, F. and Bellincampi, D. (2012) Methyl esterification of pectin plays a role during plant-pathogen interactions and affects plant resistance to diseases. *J. Plant Physiol.* **169**, 1623–1630.

Lipka, V., Dittgen, J., Bednarek, P., *et al.* (2005) Pre- and postinvasion defenses both contribute to nonhost resistance in Arabidopsis. *Science*, **310**, 1180–1183.

Liu, J., Ding, P., Sun, T., Nitta, Y., Dong, O., Huang, X., Yang, W., Li, X., Botella, J.R. and Zhang, Y. (2013) Heterotrimeric G proteins serve as a converging point in plant defense signaling activated by multiple receptor-like kinases. *Plant Physiol.* **161**, 2146–2158.

Llorente, F., Alonso-Blanco, C., Sánchez-Rodriguez, C., Jorda, L. and Molina, A. (2005) ERECTA receptor-like kinase and heterotrimeric G protein from Arabidopsis are required for resistance to the necrotrophic fungus Plectosphaerella cucumerina. *Plant J.* **43**, 165–180.

Lorek, J., Griebel, T., Jones, A.M., Kuhn, H. and Panstruga, R. (2013) The role of Arabidopsis heterotrimeric G-protein subunits in MLO2 function and MAMP-triggered immunity. *Mol. Plant Microbe Interact.* **26**, 991–1003.

Lugan, R., Niogret, M.F., Kervazo, L., Larher, F.R., Kopka, J. and Boucher-eau, A. (2009) Metabolome and water status phenotyping of Arabidopsis under abiotic stress cues reveals new insight into ESK1 function. *Plant, Cell Environ.* **32**, 95–108.

Manabe, Y., Nafisi, M., Verhertbruggen, Y., *et al.* (2011) Loss-of-function mutation of REDUCED WALL ACETYLATION2 in Arabidopsis leads to reduced cell wall acetylation and increased resistance to Botrytis cinerea. *Plant Physiol.* **155**, 1068–1078.

Maruta, N., Trusov, Y., Brenya, E., Parekh, U. and Botella, J.R. (2015) Membrane-localized extra-large G proteins and Gbg of the heterotrimeric G proteins form functional complexes engaged in plant immunity in Arabidopsis. *Plant Physiol.* **167**, 1004–1016.

McKee, L.S., Sunner, H., Anasontzis, G.E., Toriz, G., Gatenholm, P., Bulone, V., Vilaplana, F. and Olsson, L. (2016) A GH115 α-glucuronidase from Schizophyllum commune contributes to the synergistic enzymatic deconstruction of softwood glucuronoarabinoxylan. *Biotechnol. Biofuels*, **9**, 2.

Mélida, H., García-Angulo, P., Alonso-Simón, A., Encina, A., Alvarez, J. and Acebes, J.L. (2009) Novel type II cell wall architecture in dichlobenil-habituated maize calluses. *Planta*, **229**, 617–631.

Mélida, H., Sandoval-Sierra, J.V., Diéguez-Uribeondo, J. and Bulone, V. (2013) Analyses of extracellular carbohydrates in oomycetes unveil the existence of three different cell wall types. *Eukaryot. Cell*, **12**, 194–203.

Miedes, E., Vanholme, R., Boerjan, W. and Molina, A. (2014) The role of the secondary cell wall in plant resistance to pathogens. *Front. Plant Sci.* **5**, 358.

Miya, A., Albert, P., Shinya, T., Desaki, Y., Ichimura, K., Shirasu, K., Narusaka, Y., Kawakami, N., Kaku, H. and Shibuya, N. (2007) CERK1, a LysM receptor kinase, is essential for chitin elicitor signaling in Arabidopsis. *Proc. Natl Acad. Sci. USA*, **104**, 19 613–19 618.

Morales, J., Kadota, Y., Zipfel, C., Molina, A. and Torres, M.A. (2016) The Arabidopsis NADPH oxidases RbohD and RbohF display differential expression patterns and contributions during plant immunity. *J. Exp. Bot.* **67**, 1663–1676.

Niyogi, K.K., Grossman, A.R. and Björkman, O. (1998) Arabidopsis mutants define a central role for the xanthophyll cycle in the regulation of photosynthetic energy conversion. *Plant Cell*, **10**, 1121–1134.

Oldham, W.M. and Hamm, H.E. (2008) Heterotrimeric G protein activation by G-protein-coupled receptors. *Nat. Rev. Mol. Cell Biol.* **9**, 60–71.

Parker, J.E., Coleman, M.J., Szabò, V., Frost, L.N., Schmidt, R., van der Biezen, E.A., Moores, T., Dean, C., Daniels, M.J. and Jones, J.D. (1997) The Arabidopsis downy mildew resistance gene RPP5 shares similarity to the toll and interleukin-1 receptors with N and L6. *Plant Cell*, **9**, 879–894.

Pawar, P.M., Koutaniemi, S., Tenkanen, M. and Mellerowicz, E.J. (2013) Acetylation of woody lignocellulose: significance and regulation. *Front. Plant Sci.* **4**, 118.

Pawar, P.M., Derba-Maceluch, M., Chong, S.L., *et al.* (2016) Expression of fungal acetyl xylan esterase in Arabidopsis thaliana improves saccharification of stem lignocellulose. *Plant Biotechnol. J.* **14**, 387–397.

Pogorelko, G., Lionetti, V., Fursova, O., Sundaram, R.M., Qi, M., Whitham, S.A., Bogdanove, A.J., Bellincampi, D. and Zabotina, O.A. (2013) Arabidopsis and Brachypodium distachyon transgenic plants expressing Aspergillus nidulans acetylesterases have decreased degree of polysaccharide acetylation and increased resistance to pathogens. *Plant Physiol.* **162**, 9–23.

Ramos, B., Gonzalez-Melendi, P., Sanchez-Vallet, A., Sanchez-Rodriguez, C., Lopez, G. and Molina, A. (2013) Functional genomics tools to decipher the pathogenicity mechanisms of the necrotrophic fungus Plectosphaerella cucumerina in Arabidopsis thaliana. *Mol. Plant Pathol.* **14**, 44–57.

Ren, M., Venglat, P., Qiu, S., *et al.* (2012) Target of rapamycin signaling regulates metabolism, growth, and life span in Arabidopsis. *Plant Cell*, **24**, 4850–4874.

Sánchez-Rodríguez, C., Estévez, J.M., Llorente, F., Hernández-Blanco, C., Jordá, L., Pagán, I., Berrocal, M., Marco, Y., Somerville, S. and Molina, A. (2009) The ERECTA receptor-like kinase regulates cell wall-mediated resistance to pathogens in Arabidopsis thaliana. *Mol. Plant Microbe Interact.* **22**, 953–963.

Sanchez-Vallet, A., Ramos, B., Bednarek, P., López, G., Piślewska-Bednarek, M., Schulze-Lefert, P. and Molina, A. (2010) Tryptophan-derived secondary metabolites in Arabidopsis thaliana confer non-host resistance to necrotrophic Plectosphaerella cucumerina fungi. *Plant J.* **63**, 115–127.

Sánchez-Vallet, A., López, G., Ramos, B., *et al.* (2012) Disruption of abscisic acid signaling constitutively activates Arabidopsis resistance to the necrotrophic fungus Plectosphaerella cucumerina. *Plant Physiol.* **160**, 2109–2124.

Schindelin, J., Arganda-Carreras, I., Frise, E., *et al.* (2012) Fiji: an open-source platform for biological-image analysis. *Nat. Methods*, **9**, 676–682.

Schlaeppi, K. and Mauch, F. (2010) Indolic secondary metabolites protect Arabidopsis from the oomycete pathogen Phytophthora brassicae. *Plant Signal. Behav.* **5**, 1099–1101.

Schultink, A., Naylor, D., Dama, M. and Pauly, M. (2015) The role of the plant-specific ALTERED XYLOGLUCAN9 protein in Arabidopsis cell wall polysaccharide O-acetylation. *Plant Physiol.* **167**, 1271–1283.

Shpak, E.D., Berthiaume, C.T., Hill, E.J. and Torii, K.U. (2004) Synergistic interaction of three ERECTA-family receptor-like kinases controls Arabidopsis organ growth and flower development by promoting cell proliferation. *Development*, **131**, 1491–1501.

Szabados, L. and Savouré, A. (2010) Proline: a multifunctional amino acid. *Trends Plant Sci.* **15**, 89–97.

Taji, T., Ohsumi, C., Iuchi, S., Seki, M., Kasuga, M., Kobayashi, M., Yamaguchi-Shinozaki, K. and Shinozaki, K. (2002) Important roles of drought- and cold-inducible genes for galactinol synthase in stress tolerance in Arabidopsis thaliana. *Plant J.* **29**, 417–426.

Tamura, K., Peterson, D., Peterson, N., Stecher, G., Nei, M. and Kumar, S. (2011) MEGA5: molecular evolutionary genetics analysis using maximum likelihood, evolutionary distance, and maximum parsimony methods. *Mol. Biol. Evol.* **28**, 2731–2739.

Temple, B.R. and Jones, A.M. (2007) The plant heterotrimeric G-protein complex. *Annu. Rev. Plant Biol.* **58**, 249–266.

Torres, M.A. (2010) ROS in biotic interactions. *Physiol. Plant.* **138**, 414–429.

Torres, M.A., Morales, J., Sánchez-Rodríguez, C., Molina, A. and Dangl, J.L. (2013) Functional interplay between Arabidopsis NADPH oxidases and heterotrimeric G protein. *Mol. Plant Microbe Interact.* **26**, 686–694.

Trusov, Y., Rookes, J.E., Chakravorty, D., Armour, D., Schenk, P.M. and Botella, J.R. (2006) Heterotrimeric G proteins facilitate Arabidopsis resistance to necrotrophic pathogens and are involved in jasmonate signaling. *Plant Physiol.* **140**, 210–220.

Tunc-Ozdemir, M. and Jones, A.M. (2017) Ligand-induced dynamics of heterotrimeric G protein-coupled receptor-like kinase complexes. *PLoS ONE*, **12**, e0171854.

Tunc-Ozdemir, M., Urano, D., Jaiswal, D.K., Clouse, S.D. and Jones, A.M. (2016) Direct modulation of heterotrimeric G protein-coupled signaling by a receptor kinase complex. *J. Biol. Chem.* **291**, 13 918–13 925.

Ullah, H., Chen, J.G., Young, J.C., Im, K.H., Sussman, M.R. and Jones, A.M. (2001) Modulation of cell proliferation by heterotrimeric G protein in Arabidopsis. *Science*, **292**, 2066–2069.

Ullah, H., Chen, J.G., Temple, B., Boyes, D.C., Alonso, J.M., Davis, K.R., Ecker, J.R. and Jones, A.M. (2003) The beta-subunit of the Arabidopsis G protein negatively regulates auxin-induced cell division and affects multiple developmental processes. *Plant Cell*, **15**, 393–409.

Urano, D., Chen, J.G., Botella, J.R. and Jones, A.M. (2013) Heterotrimeric G protein signalling in the plant kingdom. *Open Biol.* **3**, 120–186.

Urano, D., Czarnecki, O., Wang, X., Jones, A.M. and Chen, J.G. (2015) Arabidopsis receptor of activated C kinase1 phosphorylation by WITH NO LYSINE8 KINASE. *Plant Physiol.* **167**, 507–516.

Urano, D., Miura, K., Wu, Q., Iwasaki, Y., Jackson, D. and Jones, A.M. (2016) Plant morphology of heterotrimeric G protein mutants. *Plant Cell Physiol.* **57**, 437–445.

Urbanowicz, B.R., Peña, M.J., Moniz, H.A., Moremen, K.W. and York, W.S. (2014) Two Arabidopsis proteins synthesize acetylated xylan in vitro. *Plant J.* **80**, 197–206.

Vogel, J.P., Raab, T.K., Somerville, C.R. and Somerville, S.C. (2004) Mutations in PMR5 result in powdery mildew resistance and altered cell wall composition. *Plant J.* **40**, 968–978.

Wang, H.X., Weerasinghe, R.R., Perdue, T.D., Cakmakci, N.G., Taylor, J.P., Marzluff, W.F. and Jones, A.M. (2006) A Golgi-localized hexose transporter is involved in heterotrimeric G protein-mediated early development in Arabidopsis. *Mol. Biol. Cell*, **17**, 4257–4269.

Winter, D., Vinegar, B., Nahal, H., Ammar, R., Wilson, G.V. and Provart, N.J. (2007) An "Electronic Fluorescent Pictograph" browser for exploring and analyzing large-scale biological data sets. *PLoS ONE*, **2**, e718.

Xin, Z. and Browse, J. (1998) Eskimo1 mutants of Arabidopsis are constitutively freezing-tolerant. *Proc. Natl Acad. Sci. USA*, **95**, 7799–7804.

Xin, Z., Mandaokar, A., Chen, J., Last, R.L. and Browse, J. (2007) Arabidopsis ESK1 encodes a novel regulator of freezing tolerance. *Plant J.* **49**, 786–799.

Xiong, G., Cheng, K. and Pauly, M. (2013) Xylan O-acetylation impacts xylem development and enzymatic recalcitrance as indicated by the Arabidopsis mutant tbl29. *Mol. Plant*, **6**, 1373–1375.

Yuan, Y., Teng, Q., Zhong, R. and Ye, Z.H. (2013) The Arabidopsis DUF231 domain-containing protein ESK1 mediates 2-O- and 3-O-acetylation of xylosyl residues in xylan. *Plant Cell Physiol.* **54**, 1186–1199.

Yuan, Y., Teng, Q., Zhong, R. and Ye, Z.H. (2016) Roles of Arabidopsis TBL34 and TBL35 in xylan acetylation and plant growth. *Plant Sci.* **243**, 120–130.

Zhu, H., Li, G.J., Ding, L., Cui, X., Berg, H., Assmann, S.M. and Xia, Y. (2009) Arabidopsis extra large G-protein 2 (XLG2) interacts with the Gbeta subunit of heterotrimeric G protein and functions in disease resistance. *Mol. Plant*, **2**, 513–525.

Zipfel, C., Robatzek, S., Navarro, L., Oakeley, E.J., Jones, J.D., Felix, G. and Boller, T. (2004) Bacterial disease resistance in Arabidopsis through flagellin perception. *Nature*, **428**, 764–767.